Deep Space Network

302
Antenna Positioning

Document Owner:		Approved by:	
Signature Provided	01/17/2017	Signature Provided	01/17/2017
Stephen D. Slobin Antenna System Engineer	Date	Timothy Pham Communications Systems Chief Engineer	Date
Prepared by:		**Released by:**	
Signature Provided	01/17/2017	Signature Provided	02/10/2017
Stephen D. Slobin Antenna System Engineer	Date	Christine Chang DSN Document Release Authority	Date

DSN No. **810-005, 302, Rev. D**
Issue Date: February 10, 2017
JPL D-19379; CL #17-0712

Jet Propulsion Laboratory
California Institute of Technology

Users must ensure that they are using the current version in DSN Telecommunications Link Design Handbook website:
http://deepspace.jpl.nasa.gov/dsndocs/810-005/

Review Acknowledgment

By signing below, the signatories acknowledge that they have reviewed this document and provided comments, if any, to the signatories on the Cover Page.

Signature Provided	01/17/2017	Signature Not Provided	
Jeff Berner DSN Project Chief Engineer	Date	David Rochblatt Antenna System Engineer	Date

Change Log

Rev	Issue Date	Prepared By	Affected Paragraphs	Change Summary
Initial	10/7/2004	Stephen Slobin Robert Sniffin	All	New Module
A	12/15/2009	Stephen Slobin Robert Sniffin	Many	Removed references and information related to the decommissioned 26-m antennas.
B	6/1/2010	Stephen Slobin Robert Sniffin	Table 1	Changed Azimuth Motion Limits to Travel Range and Corrected DSS-27 cable wrap center value. Eliminated the Rev. E designation for the document series.
C	02/09/2015	Stephen Slobin Christine Chang	Table 4 Figures 4,5,6,7 Section 2.1 Rev. B, Section 2.3.2 Section 2.5.2 Section 2.6	Updated MRE values – added DSS-35. Added to show wind effect on pointing loss. DSS-27 HSB antenna decommissioned. Removed, IIRV no longer supported in DSN. Expanded description of blind pointing errors. Expanded description of CONSCAN and monopulse.
D	02/10/2017	Stephen Slobin Christine Chang	Sec. 2.6.2 Table 4	Ka-band monopulse MRE at DSS-36 added. Added DSS-36 blind pointing performance. Noted that DSS-45 is decommissioned.

Contents

Illustrations

Tables

1 Introduction

1.1 Purpose

This module describes the pointing capabilities of the antennas used by the Deep Space Network (DSN) in sufficient detail to enable a telecommunications engineer to design spacecraft missions that are compatible with these capabilities.

1.2 Scope

This discussion in this document is restricted to the mechanical limitations of the antennas, their control algorithms, and the error sources that influence the ability to point the radio frequency (RF) beam in the desired direction. Wind velocity statistics that can be used to estimate the effects of wind on antenna pointing are presented in module 105. Coverage and restrictions to coverage caused by terrain masking are discussed in module 301.

2 General Information

Antenna positioning or pointing is the process of directing the antenna beam towards the desired target. The target may be a spacecraft or radio source that is producing a receivable signal. The target may also be a spacecraft other object at a known or suspected position that is not producing a signal but to which RF energy must be directed. The antenna must keep its RF beam properly aimed for the scheduled duration of the spacecraft or other observation, often referred to as a pass.

There are two types of antenna beam pointing. The first of these is blind pointing, sometimes referred to as open loop pointing, that relies on the ability to model the direction of the antenna beam in the presence of systematic and random processes. The second is closed-loop pointing that derives corrections from the received signal. Blind pointing produces larger errors, but is the only method available in the absence of a received signal or during radio science observations when the data quality would be adversely affected by closed loop positioning.

Antenna pointing is not only influenced by random errors due to wind and thermal effects, but also due to imperfect modeling of systematic pointing errors that vary unpredictably throughout the sky or along a particular path in the sky when tracking a spacecraft. Standard first-order systematic error pointing models (used for blind pointing) may not be adequate to describe “high frequency” (e.g., 2 or more cycles per 360 degrees movement in azimuth or elevation) variations in pointing. Fourth-order blind pointing models exist for all antennas and frequency bands.

2.1 Antenna Characteristics

The DSN employs three general types of antennas. At least one of each type antenna exists at each DSN complex. The antenna types are the 70-m antennas, the 34-m high-efficiency (HEF) antennas, and the 34-m beam waveguide (BWG) antennas. All of these

antennas employ an azimuth-elevation (AZ-EL) mount. The Goldstone high-speed beam waveguide (HSB) antenna (DSS-27) has been decommissioned.

The antennas are pointed by variable-rate servo systems that use the antenna pointing commands as input and the axis position encoders (azimuth and elevation) as feedback. The 70-m antennas also have a *precision mode* where the main reflector is slaved to a small hour-angle/declination instrument, referred to as the *Master Equatorial (ME)*, using optical collimation techniques. The ME is mounted at the intersection of the 70-m azimuth and elevation axes in a controlled environment and on a separate foundation to eliminate vibration and thermal effects. Servo performance is generally a function of antenna size, with higher tracking and slew rates being available from the smaller antennas. Table 1 summarizes the primary mechanical characteristics of the various antennas.

2.2 Coverage Restrictions and Servo Performance Limits

DSN antennas have restrictions to their coverage from two sources other than terrain masking. The first of these is the antenna *keyholes* – areas where coverage in not possible because the reflector would need to be positioned about the secondary (upper) axis in such a way that it would run into the primary (lower) axis or its supporting structure. The sizes of the keyholes can be inferred from the elevation motion limits given in Table 1 and are illustrated on the horizon mask charts in module 301. The second restriction occurs near the ends of the primary axis where the amount of motion required to correctly position the antenna beam exceeds the capability of the primary axis servo should the orbital path pass near an imaginary extension of the lower axis.

Azimuth-elevation antennas have an area of non-coverage directly above the antenna resulting from the fact that should a spacecraft pass directly overhead, the antenna would have to instantaneously rotate 180 degrees in azimuth to follow it. Clearly, this is not possible but, for spacecraft passing nearly overhead, the azimuth rate is finite and can be calculated from the equation.

$$r_{AZ} = \frac{r_{SC}}{\cos(EL_{Peak})} \tag{1}$$

where

r_{AZ} = the peak azimuth rate required of the antenna

r_{SC} = the cross-elevation rate of the spacecraft as seen from the antenna

EL_{Peak} = the maximum elevation reached by the spacecraft.

Table 1. DSN Antenna Mechanical Characteristics

Parameter	70-m	34-m HEF	34-m BWG
Antenna Mount	AZ-EL	AZ-EL	AZ-EL
Slew Rate, each axis (deg/s)	0.25	0.8	0.8
Minimum Tracking Rate, each axis (deg/s)	0.0001	0.0001	0.0001
Maximum Tracking Rate, each axis (deg/s)	0.25	0.4	0.4
Acceleration each axis (deg/s^2)	0.2	0.4	0.4
Deceleration (braking) each axis (deg/s^2)	2.5	5.0	5.0
Axis Encoder Resolution (mdeg)	0.021	0.021	0.021
Axis Encoder Accuracy (mdeg)	±0.171	±0.171	±0.171
Master Equatorial Axis Encoder Resolution (mdeg)	0.021	–	–
Master Equatorial Axis Encoder Accuracy (mdeg)	±0.343	–	–
Azimuth Travel Range from Wrap Center (deg)	±265	±225	±225
GDSCC Wrap Center (deg)	45	135	135
CDSCC Wrap Center (deg)	135	45	45
MDSCC Wrap Center (deg	45	135	135
Elevation Motion Limits (deg)	6 – 89.5	6 – 89.5	6 – 89.5

For spacecraft tracked at near-sidereal rates, the areas of non-coverage are not large but must be avoided by appropriate scheduling. The maximum peak spacecraft elevation is limited to 89 degrees for continuous tracking when using the 70-m antennas. For the HEF and BWG antennas, the maximum peak elevation for continuous tracking is limited to 89.4 degrees.

Formula (1) can be used for Earth-orbiter spacecraft; however, the rate of spacecraft as seen from the antenna will be a function of orbit altitude. Figure 1 illustrates the effect of orbit altitude on peak azimuth rate for several circular orbits.

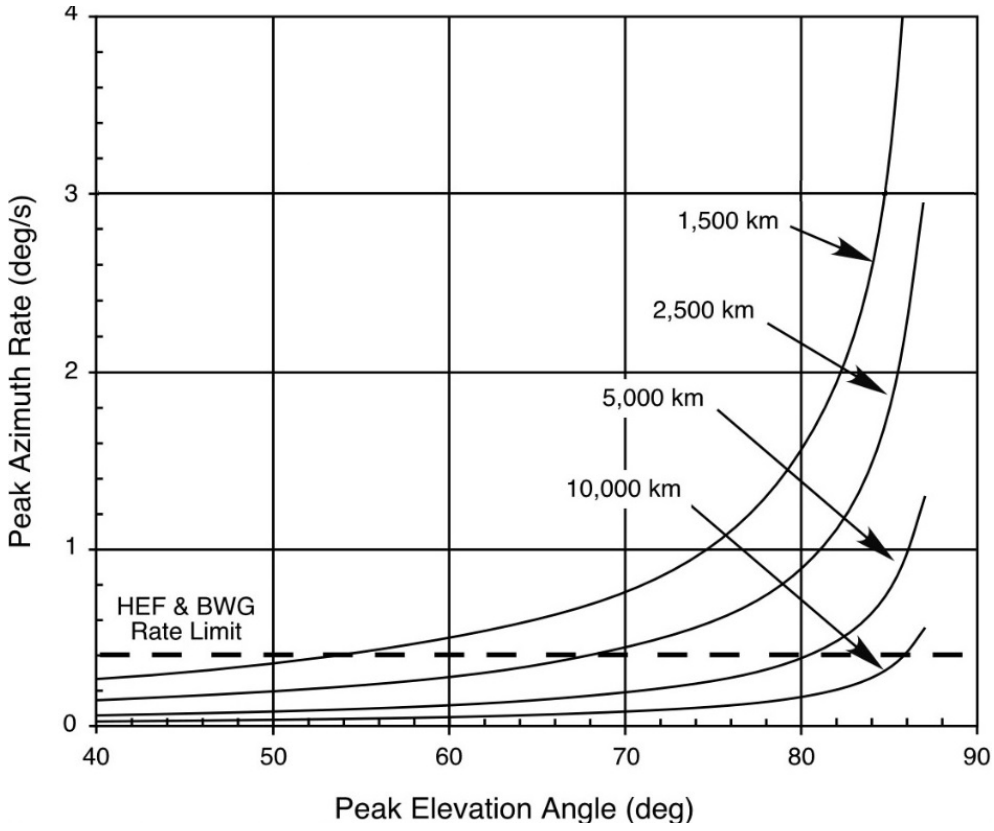

Figure 1. Azimuth Rates for Selected Circular Orbits.

2.3 Pointing Modes

DSN antennas are normally operated by aiming their RF beams in accordance with a pre-determined set of instructions referred to as antenna pointing predictions or *predicts*. The format and contents of the predicts depends on their source, the type of support being provided, and the antenna being used. In addition to predict-driven modes, there are specialized pointing modes available for the antenna type. All pointing is provided in terms of the actual

direction to the target. The antenna controller adds whatever corrections are required to compensate for the atmosphere and imperfections in the antenna response, calculates the rate at which each axis must move to reach the next point at the desired time and delivers this information to the antenna servos. Position feedback from the selected axis position encoders is constantly monitored and used to adjust the axis tracking rates.

The 34-m BWG antennas have a single predict-driven mode, the direction cosine mode. The Improved Inter-Range Vector (IIRV) mode is no longer supported in the DSN. The 34-m HEF and 70-m antennas have the direction cosine predict-driven mode. In addition, the 70-m antennas also have the precision tracking mode. Common to all antennas are the planetary and sidereal tracking modes. These pointing modes are further described below.

2.3.1 Direction Cosine Mode

Target positions are delivered to the station as a binary file of predict points, where each point contains time, target range, and topographic direction cosines (X, Y, and Z) with their 2nd and 4th differences for use in an Everett Interpolation algorithm within the antenna controller. The points may represent the location of a single spacecraft from which data is to be acquired for an entire pass, a collection of radio sources that are to be observed on a pre-determined schedule, or in the case of delta-differential one-way ranging (ΔDOR), a series of observations alternating between a spacecraft and one or more radio sources. The direction cosine predict-driven mode is commonly available for all DSN antennas.

2.3.2 Planetary Mode

Planetary mode is used to track an object with slowly varying right ascension and declination. Pointing commands are interpolated from three planetary predict points (typically one per day) entered from the control position or read from a locally-created file of at least four predict points. The points may be geocentric or topocentric and should include precession and nutation corrections. Each point contains time, right ascension, declination, and range. Parallax correction is available for use with geocentric points when a non-sidereal object (such as a planet) is to be tracked.

2.3.3 Sidereal Mode

This mode, also called Star Track Mode, is used to track a celestial object at a fixed position (fixed at least for a number of days) described by geocentric right ascension (RA) and declination (DEC) coordinates, including precession and nutation. The points may be entered from the local control position or may be read from a locally-created file containing time, RA, and DEC. A capability to boresight the antenna after arriving on point is included. The boresight algorithm performs a small cross-elevation (XEL) scan centered on the expected target location followed by a small elevation (EL) scan. Pointing corrections are estimated from signal strength measurements. This mode is mainly used for evaluating antenna performance and collecting very-long baseline interferometry (VLBI) data.

2.3.4 70-m Precision Tracking Mode

The 70-m antennas have a precision tracking mode that makes use of an instrument called the *master equatorial* (ME). The master equatorial is a 7-inch (17.8 cm) mirror

on an hour-angle/declination mount. The mount is attached to the top of a concrete and steel tower on a separate foundation in an environmentally controlled area within the antenna pedestal and alidade structure. The mirror can be positioned to better than 1 mdeg in each axis and the 70-m reflector is optically slaved to it. The precision tracking mode is available with any of the above modes but should only be used when needed because of its extra complexity.

2.4 Statistics of Pointing Errors

If an antenna has EL and XEL random pointing errors due to any number of causes that are normally (Gaussian) distributed, it can be shown that for equal EL and XEL standard deviations, σ, the radial pointing error (two dimensional) becomes Rayleigh distributed. The characteristics of the Rayleigh distribution are that the probability density function (PDF) is zero at zero pointing error, rises to a maximum value at the EL and XEL σ, and decreases with a long tail out to large values of radial pointing error. The cumulative distribution (CD) of the pointing error at a particular value is the integral of the PDF from zero to that value. The mean radial error (MRE) for the Rayleigh distribution of radial pointing errors is related to the standard deviation of the axial (XEL and EL) distributions as:

$$\mathrm{MRE} = \sqrt{\pi/2} \cdot \sigma = 1.2533\sigma \tag{2}$$

and the cumulative distribution at the MRE is 0.545. This means that 54.5% of the pointing errors are less than or equal to the MRE. Conversely, 45.5% of the pointing errors are larger than the MRE. Once the MRE is known, the radial error associated with any CD can be calculated from the properties of the Rayleigh distribution. Table 2 provides the factors by which the MRE must be multiplied to obtain the radial error at the selected CD.

Table 2. Mean Radial Error Multipliers for a Rayleigh Distribution.

CD	Mean Radial Error Multiplier	CD	Mean Radial Error Multiplier
0.0	0.000	0.6	1.080
0.1	0.366	0.7	1.238
0.2	0.533	0.8	1.431
0.3	0.673	0.9	1.712
0.4	0.806	0.95	1.953
0.5	0.939	0.98	2.232
0.545	1.000 (MRE)	0.99	2.421

Figure 2 shows a graph of the PDF and cumulative distribution function (CDF) for a Rayleigh distribution with axial (XEL and EL) σ of 3.19 mdeg, chosen to yield a mean radial error of 4.00 mdeg. Pointing performance such as this would be acceptable for a 34-m DSN antenna operating at X-band where the pointing loss (see module 104) would be less than

0.13 dB 90% of the time. It would be not be acceptable pointing for the same antenna operating at Ka-band antenna where the beamwidth is substantially smaller. The resulting Ka-band pointing loss (see module 104) would be greater than 0.7 dB 45.5% percent of the time and greater than 2 dB 10% of the time.

Figure 3 shows cumulative distributions of pointing error for values of mean radial error ranging from 2 to 20 mdeg and includes the pointing loss curves from modules 101 (70-m Telecommunications Interfaces) and 104 (34-m BWG Telecommunications Interfaces). As an example of the use of this figure, consider the inverse of the preceding example. Assuming it has been determined that a 90% probability of having no more than 2 dB of pointing loss for a Ka-band experiment is acceptable, the chart is entered from the right along the 2-dB line until it intersects the Ka-band Pointing Loss curve. The line is extended vertically to the CD = 0.9 line where it intersects the MRE = 4 curve. Thus, to accomplish the experiment with the desired pointing performance will require an antenna with an MRE capability of 4 mdeg.

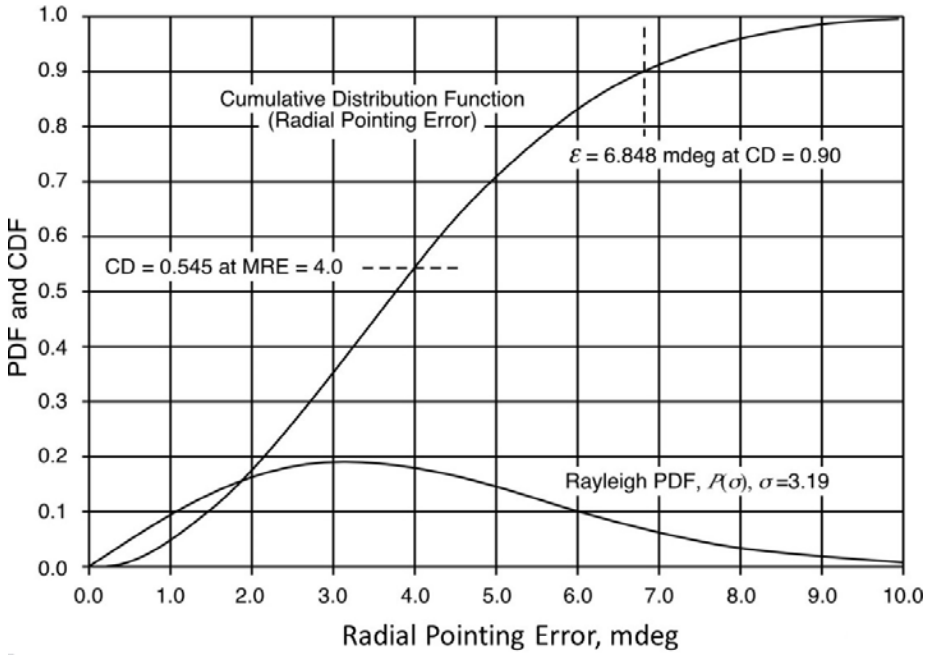

Figure 2. Rayleigh PDF and CDF for a Mean Radial Pointing Error = 4.0 mdeg.

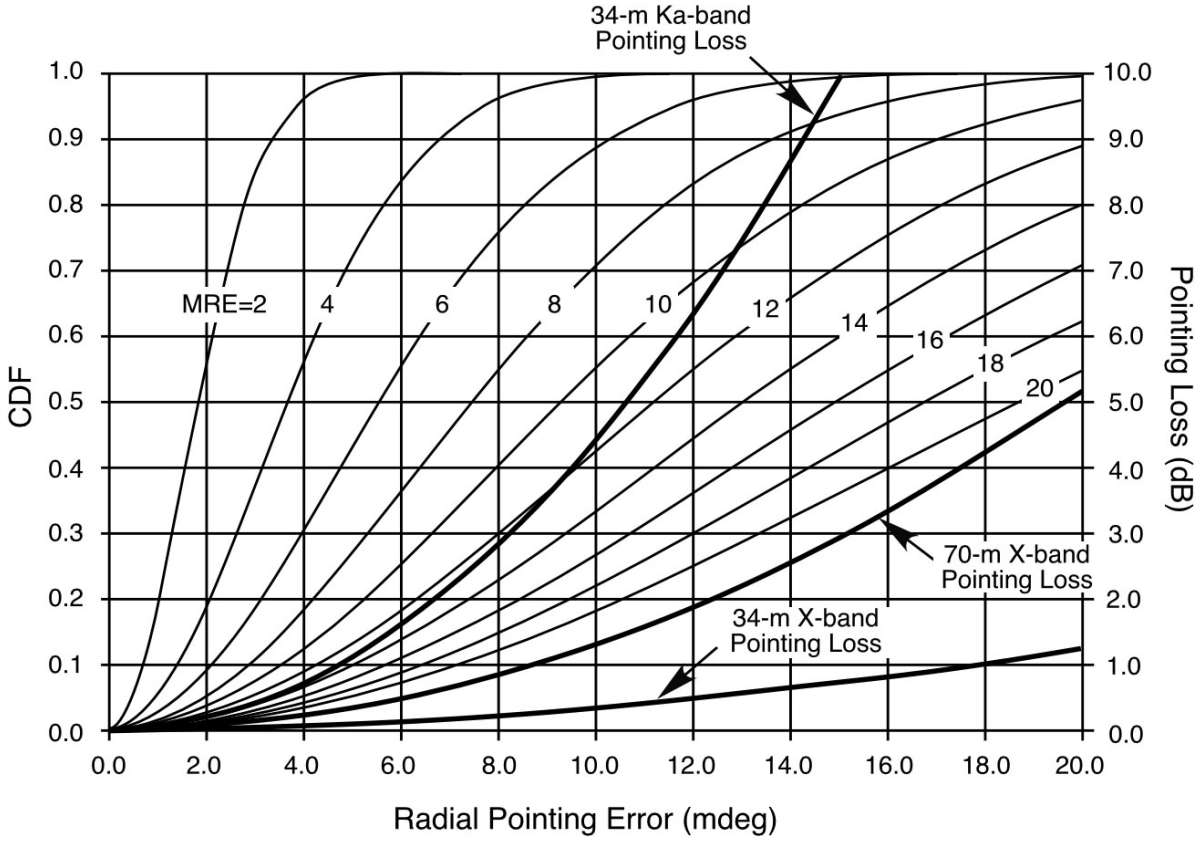

Figure 3. Cumulative Distributions of Pointing Errors for Selected MREs

2.5 Blind Pointing

Blind pointing relies on calibration and computer modeling to compensate for errors between the antenna beam direction and the direction as reported by the antenna axis position encoders. Blind pointing errors result in a pointing loss that is most severe on the BWG antennas when operating at Ka-band because of the extremely narrow beamwidth. The 70-m antennas have a relatively narrow X-band beamwidth, but this is mitigated by use of the precision tracking mode. The BWG antennas' beam waveguide tube at the center of the antenna prevents use of a master equatorial, and there are additional error sources. The BWG error sources, their magnitude, and the degree to which they can be reduced by modeling are tabulated in Table 3 and discussed in the following paragraphs.

Table 3. 34-m BWG Antenna Pointing Error Sources

Error Source	Estimated Size (mdeg)	Correction Method	Residual Error (mdeg)
Atmospheric refractivity	83 at EL = 10°	Surface weather model	0.8, 1σ at EL=10°
Gravity deformation of dish and quadripod	100, EL (max)	Subreflector lookup table	5 – 10 P-P (≅ 6σ)
Systematic errors	100, EL (max)	12 term, first order trigonometric model	1 – 8 (range)
Azimuth track level	8 P-P (≅ 6σ	Lookup table	0.3 XEL, 0.1 EL
Azimuth encoder gear noise	0.44, 1σ	Uncorrected	0.44, 1σ
Elevation encoder	0.2	Uncorrected	0.2, 1σ
Thermal deformation	8 P-P (≅ 6σ EL & XEL)	Uncorrected	8 P-P (≅ 6σ
Wind displacement of foundation	1.1 (30 mph wind)	Uncorrected	1.1 (30 mph wind)
Wind distortion of structure	6 – 9 (30 mph wind)	Uncorrected	6 – 9 (30 mph wind)
Calibration measurements	1, 1σ	Uncorrected	1, 1σ
Mean pointing error (without wind)			2.3 – 8.4 (range)
Mean pointing error (with 30 mph wind)			6.5 – 12.4 (range)

2.5.1 Pointing Corrections

2.5.1.1 Atmospheric Refraction Correction

The antenna controller uses local surface weather measurements to calculate and apply a pointing correction in elevation to compensate for atmospheric refraction. The weather data normally is provided from a local weather station but may be manually entered, if necessary.

2.5.1.2 Gravity Deformation Correction

The main reflector and the quadripod structure that supports the subreflector change shape slightly when the antenna moves in elevation. Because of this, the subreflector must be moved continuously during a pass in both the up and down as well as the in and out directions to optimize the gain. The up-down component of the motion causes a shift in antenna

pointing referred to as *squint*. This is compensated for by a squint correction algorithm that adjusts the elevation pointing depending on how far the subreflector has been moved.

2.5.1.3 Systematic Error Correction

All antennas, no matter how well they are designed and how carefully they are built, have certain repeatable pointing errors that can be measured by referencing well-known radio sources. Among the causes for these errors are imperfections such as angle-encoder offsets, azimuth axis tilt, gravitational flexure, axis skew, structure aging, etc. The DSN models these using constants and spherical harmonic functions of the antenna pointing angle in what is called a first-order pointing model. This model works reasonably well over the entire sky at S-band and X-band. However, experiments requiring extremely accurate pointing can benefit by special calibrations and adjusting the model for optimum performance in the portion of the sky where the experiment will occur. Antenna calibrations are performed periodically and the best model for the planned activity is always used.

The addition of Ka-band to the network has made the first order model inadequate as an all-sky model. As a result, a 4^{th} order systematic error model has been developed to handle pointing variations that are not directly traceable to physical imperfections in the antenna. More frequent calibration and possible use of different models for day and night operation are also being investigated to improve Ka-band pointing.

2.5.1.4 Azimuth Track Level Compensation

The BWG antenna azimuth tracks are composed of eight, precision-machined segments. Extremely small irregularities in the track, coupled with the four-wheeled rectangular support structure for the antenna, result in a 32-node signature that is more complex than can be modeled by the 1^{st} order or 4^{th} order systematic error correction model. The antenna controller employs a lookup table and applies appropriate corrections to both elevation and azimuth axes.

2.5.2 Measured Blind Pointing Performance of DSN Antennas

Table 4 presents measured X-band blind-pointing pointing performance of DSN antennas. S-band pointing is provided only for DSS-36. X-band pointing models are good enough to be used for S-band, due to the much larger S-band beamwidth. The blind pointing performance presented here is deduced from the pointing errors measured at X-band by CONSCAN and at Ka-band by monopulse (see below) during tracks on numerous spacecraft over a period of 3 to 9 months during 2014, and at DSS-36 during 2016. Although the pointing was maintained nearly perfectly on the spacecraft by use of the closed-loop systems, the running sum of the individual pointing corrections gives a measure of how much the blind pointing error varies over a track − in other words, how far the commanded antenna position varies from the actual spacecraft position. Additionally, reported pointing calibrations at the Madrid station include measurements made by ACME (Antenna Calibration and Measurement Equipment) on radio sources.

Table 4. Measured Blind Pointing Performance of DSN Antennas

Antennas	Mean Radial Error, mdeg	Remarks (see NOTE)
70-Meter		
DSS-14, Goldstone	3.2	X-band
DSS-43, Canberra	2.2	X-band
DSS-63, Madrid	2.9	X-band
	2.0	X-band, ACME
34-Meter HEF		
DSS-15, Goldstone	5.4	X-band
DSS-45, Canberra	See NOTE	
DSS-65, Madrid	6.0	X-band
	4.7	X-band, ACME
34-Meter BWG		
DSS-24, Goldstone	4.4	X-band
DSS-25, Goldstone	3.5	X-band
	2.7	Ka-band
DSS-26, Goldstone	5.3	X-band
	3.1	Ka-band
DSS-34, Canberra	5.9	X-band
	3.9	Ka-band
DSS-35, Canberra	7.7	X-band, preliminary
	2.5-3.4	Ka-band
DSS-36, Canberra	6.3	S-band
	5.8	X-band
	3.4	Ka-band
DSS-54, Madrid	3.2	X-band
	4.4	X-band, ACME
	3.2	Ka-band
DSS-55, Madrid	3.9	X-band
	3.5	X-band, ACME
	4.2	Ka-band

NOTE: X-band = CONSCAN measurements of blind pointing
Ka-band = monopulse measurements of blind pointing
ACME = Antenna Calibration and Measurement Equipment
DSS-45 decommissioned as of October 2016.

2.6 Closed-loop Pointing

Closed-loop pointing relies on the signal being received to provide corrections for antenna pointing. The DSN employs two methods of closed-loop pointing, CONSCAN and monopulse. Table 4 (above) presents the deduced blind pointing performance of DSN antennas as determined by closed-loop CONSCAN (X-band) and monopulse (Ka-band) pointing measurements.

2.6.1 CONSCAN

CONSCAN is available on all 70-m and 34-m antennas. It consists of performing a circular scan (as seen looking at the spacecraft) with the center at the predicted source position and a radius that reduces the received signal level by a small amount, typically 0.1 dB. If the target is at the expected location and antenna pointing model is perfect, no variation in the received signal level will be detected, although it will be down 0.1 dB from the maximum possible received signal level. If the initial pointing is imperfect or the target is not at the predicted location, each CONSCAN cycle will see a variation in amplitude from which the radial error and clock angle of the mis-pointing can be calculated. The typical time for a CONSCAN cycle is 120 seconds and the pointing is corrected after each cycle. The process is repeated continuously during the pass. Various amounts of CONSCAN "gain" can be applied for making the pointing correction, ranging from 0 (no correction applied) to 1 (full detected correction applied). A gain of less than 1 is usually applied to reduce the effect of noise during the CONSCAN cycle. This results in some time delay (perhaps 20 minutes) before fully corrected pointing is obtained.

CONSCAN is available at all frequency bands but is usually not necessary at S-band and is not recommended for Ka-band, since monopulse (see below) is usually available.

The relatively long CONSCAN cycle coupled with the much more severe Ka-band atmospheric effects can provide misleading information to the pointing correction algorithm resulting in the antenna being driven off-point.

The mean pointing error (used for estimating pointing loss) using CONSCAN should be considered as the 0.1 dB point on the antenna pattern for the antenna and frequency in question. For a 34-meter antenna at X-band, this value is 6 mdeg and for a 70-meter antenna at X-band it is 3 mdeg. Considering CONSCAN pointing to be Rayleigh distributed, the pointing error for various CDs can be calculated from Figure 3. Antenna beam patterns for the various DSN antennas are given in modules 101 through 104.

The most critical pointing requirements in the DSN are for the use of Ka-band on the 34-m BWG antennas. This is because the half-power beamwidth is about 0.017 degrees, half the width of the X-band beam on the 70-m antennas. Tracking results using CONSCAN indicate that the center of the CONSCAN circle can typically be kept pointed to within 6 mdeg of a spacecraft at X-band, and somewhat less at Ka-band.

Figure 4 shows the X-band pointing errors as measured by CONSCAN during a Kepler spacecraft track on the DSS-34 BWG antenna in August, 2012. Wind speeds up to about 45 km/hr were experienced during the track, and it is felt that significant pointing errors resulted. A straight-line fit through the data indicates a mean pointing error of as much as 0.004 degrees for 45 km/hr wind speed, although individual points are as much as 0.008 degrees. Each radial pointing error is the resulting measurement of one two-minute CONSCAN circle. The average X-band pointing loss over the CONSCAN cycle is small, less than 0.3 dB for the points shown in Figure 5.

Assuming that the pointing errors determined using Ka-band CONSCAN would be the same as what were measured at X-band, the average pointing losses over the Ka-band CONSCAN cycle are shown in Figure 6. In this case, at 50 km/hr the straight-line fit gives 1.0 dB, although individual points are as much as 2.8 dB. Because of the wider X-band beamwidth, it is felt that the X-band CONSCAN measurements are noisier (in degrees) than what would be experienced at Ka-band, so estimates of the maximum Ka-band pointing losses are probably exaggerated to some degree.

There may be some conditions under which it might be necessary to use X-band CONSCAN while tracking at both X- and Ka-bands. Possibilities include unavailability of Ka-band monopulse (Section 2.6.2), or gusty wind conditions which introduce excessive pointing "noise" into the Ka-band CONSCAN cycle. For the case of Ka-band tracking using X-band CONSCAN (for coincident X- and Ka-band beams), the Ka-band losses will be greater than those using Ka-band CONSCAN, as the Ka-band beam is "dragged around" in the X-band CONSCAN process, and thus is generally further away from the spacecraft than it would be using Ka-band CONSCAN alone. In this case the Ka-band pointing losses are shown in Figure 7, and individual points are as large as 3.4 dB, with a minimum of 1.44 dB. The straight-line fit gives an average pointing loss over the CONSCAN cycle of about 2.0 dB at a wind speed of 50 km/hr.

Each pointing loss value shown in the figures is the average pointing loss over the two-minute CONSCAN cycle; thus there is a portion of the CONSCAN cycle where the pointing loss is significantly worse than the average, which might result in the spacecraft signal being lost. The straight-line fits are not intended to suggest a model, but rather to indicate the trends of pointing error and loss as a function of wind speed.

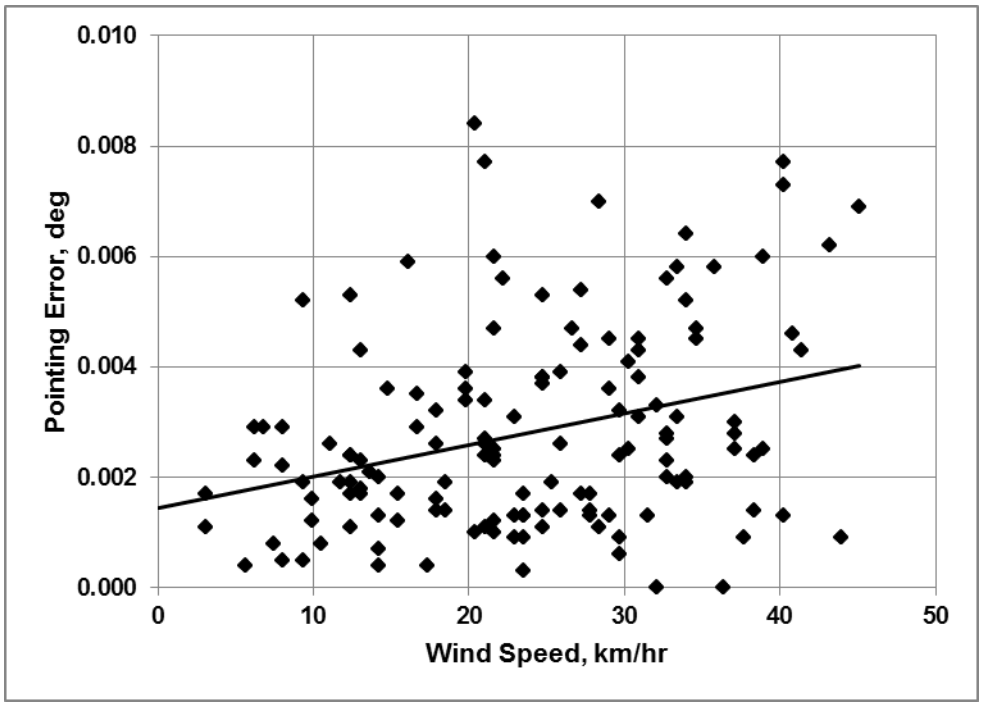

Figure 4. 34-m BWG Antenna X/Ka-band Pointing Error vs. Wind Speed

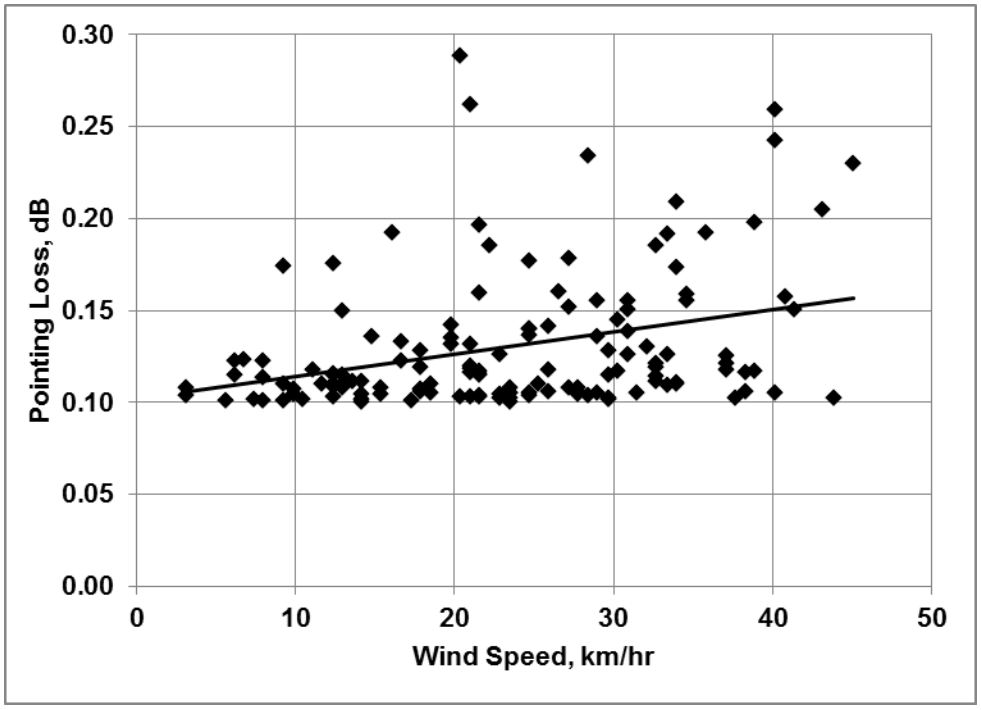

Figure 5. X-band CONSCAN Average Pointing Loss vs. Wind Speed

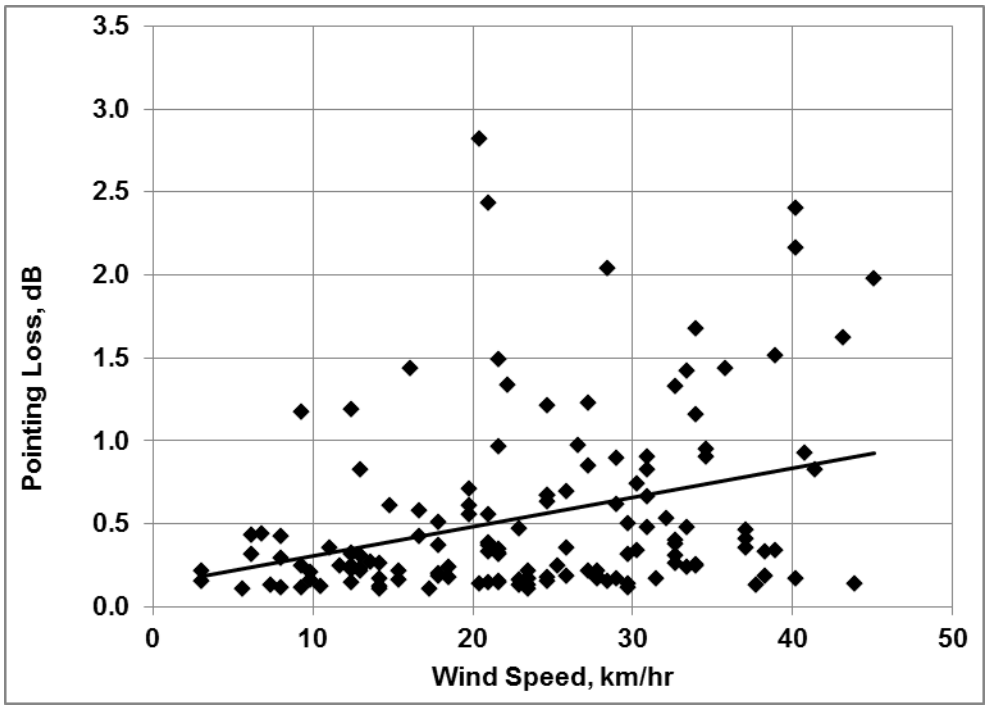

Figure 6. Ka-band CONSCAN Average Pointing Loss vs. Wind Speed

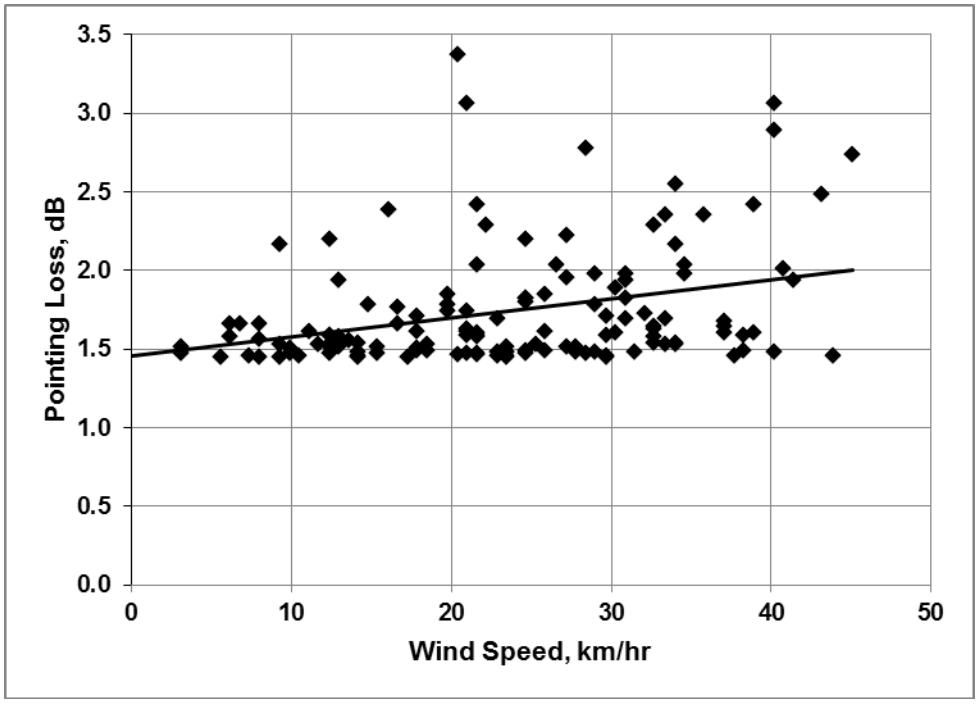

Figure 7. Ka-band Average Pointing Loss using X-band CONSCAN vs. Wind Speed

2.6.2 Monopulse

Monopulse is a technique for extracting pointing information from the phase of the received signal while maintaining the source at the peak of the antenna pattern. This technique relies on the presence of a carrier signal to provide a reference for the error channel(s). As a result, it is not suitable for suppressed carrier signals or radio sources.

The monopulse capability is available to support deep space Ka-band (32-GHz) at DSS-25, DSS-26, DSS-34, DSS-35, DSS-36, DSS-54, and DSS-55. The Ka-band feeds of these 34-m BWG antennas include a cryogenically cooled TE_{21} mode coupler that extracts a signal whose phase, with respect to the main beam signal, indicates the direction of the target with respect to the center of the beam and whose amplitude indicates the angular displacement from the beam center. The advantage of such a system over a conventional amplitude monopulse system is that only a single receiver channel is required for the error signal as opposed to two. The monopulse receiver measures the phase and amplitude of the signal in the error channel, calculates elevation and cross-elevation corrections, and forwards this information to the antenna controller 25 times a second. The antenna controller translates the errors into the local antenna coordinate system, integrates them, and applies the corrections to the predicted azimuth and elevation positions. During most Ka-band tracks using monopulse the pointing is maintained to with 2 mdeg, resulting in a maximum pointing loss of less than 0.2 dB. Monopulse pointing at DSS-36 was measured to be 1.5 mdeg MRE. Monopulse used at Ka-band is also used to determine the blind pointing errors for the 34-meter BWG antennas.For initial acquisition using blind pointing, monopulse should be able to "pull-in" when the pointing is within about 10 mdeg. For larger pointing errors and/or low signal to noise ratios (SNRs), CONSCAN is used to get on target.

For extremely high signal-to-noise ratios (SNR > 40 dB-Hz), the monopulse system is capable of pointing the antenna within 1 mdeg of a stationary target. As SNR decreases, this performance is degraded by servo jitter resulting from noise in the selected servo bandwidth. A study has shown that the mean radial error using monopulse varies with SNR approximately as

$$MRE = 0.2 + 12e^{-0.13SNR} \text{ , mdeg} \tag{3}$$

where SNR is the monopulse signal-to-noise ratio, dB-Hz (signal in the main channel divided by noise in the error channel). For example, for SNR = 20 dB-Hz, MRE = 1.1 mdeg. SNRs below 10 dB-Hz will probably yield unacceptably poor pointing performance.

2.7 Beam Alignment

Most DSN antennas that support more than one frequency accomplish this by having multiple feedhorns. The exceptions to this are the 34-m HEF antennas that have a single S- and X-band coaxial feedhorn and the BWG antennas (with the exception of DSS-25) where there is a coaxial X- and Ka-band feedcone. When multiple feedcones are used, it is likely that there will be a small misalignment between the peak of the two antenna beams. However, if good pointing is achieved at the higher frequency, it virtually guarantees nearly perfect performance at the lower frequency due to the larger beamwidth. For example on the DSS-43, 70-m antenna

(Canberra), the S- and X-band beams have a pointing difference of about 4 mdeg in the EL direction. Because the S-band beam has a half-power beamwidth of about 118 mdeg, perfect pointing at X-band would give an S-band pointing loss of less than 0.02 dB.

2.8 X-band Beam Shift on 70-m Antennas

The 70-meter antennas have an S/X dichroic plate that is retractable to provide an X-band only low-noise mode. There is an 8.5 mdeg (approximately) beam movement in the negative XEL direction (to the left, when looking outward from the antenna) when it is retracted. Separate systematic error models are maintained for each position of the dichroic plate and are selected automatically by the antenna controller.

2.9 DSS-25 Ka-band Transmit Aberration Correction

The extremely narrow beamwidth at Ka-band requires that the DSS-25 Ka-band uplink signal be aimed at the RA and DEC where the spacecraft will be when the signal arrives, while simultaneously receiving a signal that left the spacecraft one light-time previously. This is accommodated by mounting the Ka-band transmit feed on a movable X-Y platform that can displace the transmitted beam as much as 30 mdeg from the received beam. The reduction in gain caused by the feed not being located at the optimum focus of the antenna is discussed in module 104.